FRONTIERS OF PHYSICS

RESEARCH ARTICLE
Volume 17 / Issue 6 / 61502 / 2022

Transfer of quantum entangled states between superconducting qubits and microwave field qubits

Tong Liu[1], Bao-Qing Guo[1], Yan-Hui Zhou[1], Jun-Long Zhao[1], Yu-Liang Fang[1], Qi-Cheng Wu[1], Chui-Ping Yang[1,2,†]

1 Quantum Information Research Center, Shangrao Normal University, Shangrao 334001, China
2 Department of Physics, Hangzhou Normal University, Hangzhou 311121, China
Corresponding author. E-mail: †yangcp@hznu.edu.cn
Received December 10, 2021; accepted March 26, 2022

ABSTRACT

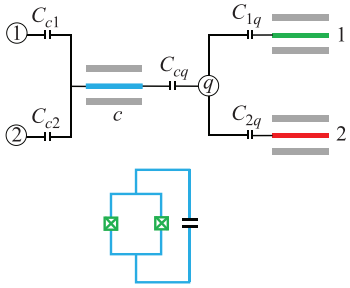

Transferring entangled states between matter qubits and microwave-field (or optical-field) qubits is of fundamental interest in quantum mechanics and necessary in hybrid quantum information processing and quantum communication. We here propose a way for transferring entangled states between superconducting qubits (matter qubits) and microwave-field qubits. This proposal is realized by a system consisting of multiple superconducting qutrits and microwave cavities. Here, "qutrit" refers to a three-level quantum system with the two lowest levels encoding a qubit while the third level acting as an auxiliary state. In contrast, the microwave-field qubits are encoded with coherent states of microwave cavities. Because the third energy level of each qutrit is not populated during the operation, decoherence from the higher energy levels is greatly suppressed. The entangled states can be deterministically transferred because measurement on the states is not needed. The operation time is independent of the number of superconducting qubits or microwave-field qubits. In addition, the architecture of the circuit system is quite simple because only a coupler qutrit and an auxiliary cavity are required. As an example, our numerical simulations show that high-fidelity transfer of entangled states from two superconducting qubits to two microwave-field qubits is feasible with present circuit QED technology. This proposal is quite general and can be extended to transfer entangled states between other matter qubits (e.g., atoms, quantum dots, and NV centers) and microwave- or optical-field qubits encoded with coherent states.

Keywords tranferring entangled states, superconducting qubits, microwave field qubits, coherent states, circuit QED

1 Introduction

The realm of circuit QED (quantum electrodynamics) investigates the light-matter interaction between superconducting qubits (*SC* qubits) and microwave cavities. It is known that circuit QED is one of the most promising well-established platforms for achieving large-scale quantum computing and quantum information processing (QIP) [1–6]. A superconducting circuit system exhibits excellent scalability, flexibility, and tunability, in which very strong coupling can be realized between SC qubits and microwave cavities [7, 8].

For SC qubits, their coherence times have been significantly improved with state-of-the-art Josephson junction technology, and a coherence time $\sim$ 2 ms [9] of an SC qubit has been experimentally reported. Over the past twenty years, many theoretical methods for transferring quantum states between SC qubits have been proposed in circuit QED (e.g., Refs.[1, 2, 10–14]). In experiments, quantum state transfer between two SC qubits via a superconducting cavity [15] and transfer of states in a chain of SC qubits [16] have been demonstrated. In addition, multipartite entangled states are central resources and have many applications in QIP and quantum communication. Up to now, various kinds of entangled states of SC qubits (e.g., GHZ states, W states, and cluster states)

Higher Education Press

https://doi.org/10.1007/s11467-022-1166-1

have been prepared in theory [17–31]. The generation of entangled states with 10–20 SC qubits has been experimentally achieved in circuit QED [32–34].

On the other hand, QIP with superconducting microwave cavities has also drawn much attention. Recently, a microwave cavity with the photon lifetime ~ 2 s has been experimentally realized [35]. Compared with SC qubits, microwave photons contained by a superconducting cavity or resonator can have longer coherence time, making them particularly suitable as good quantum memories. In addition, the microwave photon states of cavities can be used to encode quantum information in high-dimensional Hilbert spaces. A large number of schemes have been presented for generating different kinds of entangled states of microwave cavities [36–51]. Experimentally, Fock states [52], Schrödinger cat states [53], two-mode cat states [54], and NOON states [55] have been created in circuit QED.

In this paper, we present a way to transfer quantum entangled states from a group of SC qubits to another group of microwave-field qubits. For simplicity, we here denote "*microwave–field qubits*" as MF qubits. The state transfer is described as

$$\begin{aligned} &a|g\rangle_1|g\rangle_2\cdots|g\rangle_N+b|e\rangle_1|e\rangle_2\cdots|e\rangle_N\\ &\rightarrow a|\alpha\rangle_{c_1}|\alpha\rangle_{c_2}\cdots|\alpha\rangle_{c_N}+b|-\alpha\rangle_{c_1}|-\alpha\rangle_{c_2}\cdots|-\alpha\rangle_{c_N}, \end{aligned} \tag{1}$$

where the SC qubits are encoded with two energy levels $|g\rangle$ and $|e\rangle$ of qubits, while the MF qubits are encoded with coherent states $|\alpha\rangle$ and $|-\alpha\rangle$ of cavities. In Eq. (1), a and b are the normalized complex numbers, satisfying $|a|^2+|b|^2=1$. When $a=b=1/\sqrt{2}$, the transferred state is a maximally entangled state. For two qubits, the entangled states in Eq. (1) are Bell states, which have wide applications in quantum communication. For three qubits or more, the entangled states in Eq. (1) are the well-known GHZ states, which play a central role in quantum teleportation [56], error correction [57], quantum metrology [58], etc..

Our proposal has these distinguishing advantages: (i) The entangled states can be deterministically transferred because measurement on the states of SC qubits or cavities is not needed. (ii) The operation time is independent of the number of SC qubits or MF qubits. (iii) Due to the third energy level of each qutrit is not populated during the operation, the decoherence of qutrit's higher energy levels is greatly minimized, and (iv) The architecture of the circuit system is compact and simple because only a coupler qutrit and an auxiliary cavity are required. In addition, this proposal is quite general and can be extended to transfer entangled states between other matter qubits (e.g., atoms, quantum dots, and NV centers) and microwave- or optical-field qubits encoded with coherent states. To the best of our knowledge, this work is the first to demonstrate that based on circuit QED, the entangled states of SC qubits can be transferred onto MF qubits deterministically.

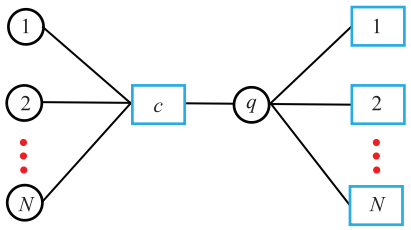

Fig. 1 Diagram of setup consisting of superconducting qutrits (black circles) $q, 1, 2, 3, \cdots, N$, and microwave cavities (blue rectangles) $c, 1, 2, 3, \cdots, N$. The qutrits are capacitively or inductively coupled to their cavities.

We believe that this work is of interest. First, the entangled coherent states are very important in quantum information science and technology. For example, the entangled coherent states can be widely used in quantum teleportation [59], quantum computation [60], quantum metrology [61], and error correction [62, 63]. Moreover, they have application in the demonstration of the Bell-type inequality violations [64]. Second, transferring entangled states between SC qubits and MF qubits may be necessary and important in the hybrid QIP. For instance, in a hybrid QIP based on SC qubits and MF qubits, entanglement transfer may be necessary between SC-qubit-based quantum processors and MF-qubits-based quantum processors. Lastly, SC qubits are matter qubits, which are different from microwave-field qubits. Transferring entangled states between matter qubits and microwave-field qubits is of fundamental interest in quantum mechanics. Recently, bosonic codes are particularly appealing and play important roles in QIP and quantum computing [65, 66]. There exist three kinds of significant bosonic codes, e.g., Gottesman–Kitaev–Preskill (GKP) [67], cat [68], and binomial codes [69, 70]. Our work may have potential applications in bosonic codes.

This paper is organized as follows. In Section 2, we introduce the basic theory. In Section 3, we show how to transfer entangled states between SC qubits and MF qubits. In Section 4, we discuss the possible experimental implementation of our proposal and numerically evaluate the operational fidelity for transferring entangled states from two SC qubits to two MF qubits. A concluding summary is given in Section 5.

2 Basic theory

Consider a system consisting of a microwave cavity c, a superconducting qutrit q, N superconducting qutrits $(1, 2, 3, \cdots, N)$, and N microwave cavities $(1, 2, 3, \cdots, N)$, as shown in Fig. 1. The three levels of the qutrit q are labeled as $|g\rangle_q$, $|e\rangle_q$, $|f\rangle_q$, while the three levels of the qutrit l are labeled as $|g\rangle_l$, $|e\rangle_l$, $|f\rangle_l$ $(l=1,2,3,\cdots,N)$ (Fig. 2). In the following subsections, we will give an introduction

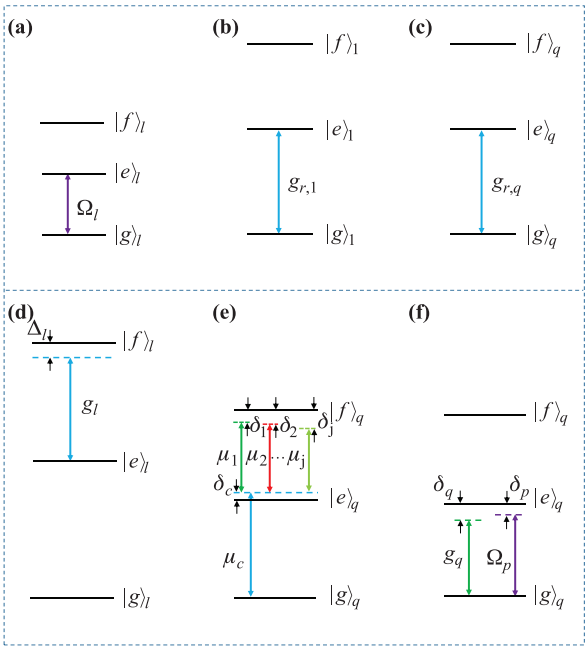

Fig. 2 **(a)** Resonant interaction between a microwave pulse and the $|g\rangle_l \leftrightarrow |e\rangle_l$ transition of qutrit l ($l = 2, 3, \cdots, N$) with the Rabi frequency Ω_l. **(b)** Resonant interaction between cavity c and the $|g\rangle_1 \leftrightarrow |e\rangle_1$ transition of qutrit 1 with coupling strength $g_{r,1}$. **(c)** Resonant interaction between cavity c and the $|g\rangle_q \leftrightarrow |e\rangle_q$ transition of qutrit q with coupling strength $g_{r,q}$. **(d)** Cavity c is dispersively coupled to the $|e\rangle_l \leftrightarrow |f\rangle_l$ transition of qutrit l ($l = 2, 3, \cdots, N$) with coupling strength g_l and detuning $\Delta_l > 0$. **(e)** Cavity c is dispersively coupled to the $|g\rangle_q \leftrightarrow |e\rangle_q$ transition of qutrit q with coupling strength μ_c and detuning $\delta_c < 0$, while cavity j ($j = 1, 2, 3, \cdots, N$) is dispersively coupled to the $|e\rangle_q \leftrightarrow |f\rangle_q$ transition of qutrit q with coupling strength μ_j and detuning δ_{c_j} (not shown) $= \delta_c + \delta_j > 0$. **(f)** Cavity 1 is dispersively coupled to the $|g\rangle_q \leftrightarrow |e\rangle_q$ transition of qutrit q with coupling strength g_q and detuning $\delta_q > 0$. Meanwhile, a microwave pulse is dispersively coupled to the $|g\rangle_q \leftrightarrow |e\rangle_q$ transition of qutrit q with the Rabi frequency Ω_p and detuning $\delta_p = \omega_{eg,q} - \omega_p > 0$. In (a–f), the level spacings of qutrits are different, which is required to have the qutrits coupled to or decoupled from cavities during the entangled state transfer (described in Section 3).

to the state evolution under a few types of interactions.

2.1 Pulse–qutrit resonant interaction

Assume that a microwave pulse is resonant with the $|g\rangle_l \leftrightarrow |e\rangle_l$ transition of qutrit l ($l = 2, 3, \cdots, N$), as shown in Fig. 2(a). In the interaction picture and after a rotating-wave approximation (RWA), the Hamiltonian is

$$H_1 = \Omega_l(\mathrm{e}^{-\mathrm{i}\phi_l}\sigma_{eg,l}^{+} + h.c.), \tag{2}$$

where $\sigma_{eg,l}^{+} = |e\rangle_l\langle g|$ is the raising operator between $|g\rangle_l \leftrightarrow |e\rangle_l$ transition of qutirt l ($l = 2, 3, \cdots, N$), Ω_l and ϕ_l are the Rabi frequency and the initial phase of the pulse. Under the Hamiltonian (2), the state rotations are given by

$$\begin{aligned} |g\rangle_l &\to \cos(\Omega_l t)|g\rangle_l - \mathrm{i}\mathrm{e}^{-\mathrm{i}\phi_l}\sin(\Omega_l t)|e\rangle_l, \\ |e\rangle_l &\to -\mathrm{i}\mathrm{e}^{\mathrm{i}\phi_l}\sin(\Omega_l t)|g\rangle_l + \cos(\Omega_l t)|e\rangle_l. \end{aligned} \tag{3}$$

2.2 Cavity–qutrit resonant interaction

Suppose that cavity c is resonant with the $|g\rangle_1 \leftrightarrow |e\rangle_1$ transition of qutrit 1 with coupling strength $g_{r,1}$, as illustrated in Fig. 2(b). The Hamiltonian in the interaction picture and after the RWA is

$$H_2 = g_{r,1}(\hat{a}_c\sigma_{eg,1}^{+} + h.c.), \tag{4}$$

where $\hat{a}_c$ is the photon annihilation operator for cavity c, and $\sigma_{eg,1}^{+} = |e\rangle_1\langle g|$.

Under the Hamiltonian (4), one obtains the state evolution

$$\begin{aligned} |g\rangle_1|1\rangle_c &\to \cos(g_{r,1}t)|g\rangle_1|1\rangle_c - \mathrm{i}\sin(g_{r,1}t)|e\rangle_1|0\rangle_c, \\ |e\rangle_1|0\rangle_c &\to \cos(g_{r,1}t)|e\rangle_1|0\rangle_c - \mathrm{i}\sin(g_{r,1}t)|g\rangle_1|1\rangle_c, \end{aligned} \tag{5}$$

where $|0\rangle_c$ and $|1\rangle_c$ are the vacuum and single photon states of cavity c, respectively.

Now assume that cavity c is resonant with the $|g\rangle_q \leftrightarrow |e\rangle_q$ transition of qutrit q with coupling strength $g_{r,q}$ [Fig. 2(c)]. Similarly, one can obtain the Hamiltonian

$$H_3 = g_{r,q}(\hat{a}_c\sigma_{eg,q}^{+} + h.c.), \tag{6}$$

and the state evolution

$$\begin{aligned} |g\rangle_q|1\rangle_c &\to \cos(g_{r,q}t)|g\rangle_q|1\rangle_c - \mathrm{i}\sin(g_{r,q}t)|e\rangle_q|0\rangle_c, \\ |e\rangle_q|0\rangle_c &\to \cos(g_{r,q}t)|e\rangle_q|0\rangle_c - \mathrm{i}\sin(g_{r,q}t)|g\rangle_q|1\rangle_c, \end{aligned} \tag{7}$$

where $\sigma_{eg,q}^{+} = |e\rangle_q\langle g|$.

2.3 Cavity–qutrit dispersive interaction

Assume that cavity c is dispersively coupled to the $|e\rangle_l \leftrightarrow |f\rangle_l$ transition of qutrit l ($l = 2, 3, \cdots, N$) with coupling strength g_l and detuning $\Delta_l = \omega_{fe,l} - \omega_c > 0$, as depicted in Fig. 2(d). Here, $\omega_{fe,l}$ is the $|e\rangle_l \leftrightarrow |f\rangle_l$ transition frequency of qutrit l and ω_c is the frequency of cavity c. In the interaction picture and after making the RWA, the Hamiltonian is

$$H_4 = \sum_{l=2}^{N} g_l(\mathrm{e}^{\mathrm{i}\Delta_l t}\hat{a}_c\sigma_{fe,l}^{+} + h.c.), \tag{8}$$

where $\sigma_{fe,l}^{+} = |f\rangle_l\langle e|$ is the raising operator between the $|e\rangle_l \leftrightarrow |f\rangle_l$ transition of qutirt l ($l = 2, 3, \cdots, N$).

Applying the large-detuning conditions $\Delta_l \gg g_l$, one can obtain the effective Hamiltonian [71–73]

$$H_{e1} = \sum_{l=2}^{N} \lambda_l(\hat{a}_c\hat{a}_c^{\dagger}|f\rangle_l\langle f| - \hat{a}_c^{\dagger}\hat{a}_c|e\rangle_l\langle e|)$$

$$+\sum_{l\neq l'=2}^{N}\lambda_{ll'}(|f\rangle_l\langle e|\otimes|e\rangle_{l'}\langle f|+|e\rangle_l\langle f|\otimes|f\rangle_{l'}\langle e|), \tag{9}$$

where $\lambda_l=\frac{g_l^2}{\Delta_l}$, $\lambda_{ll'}=\frac{g_l g_{l'}}{2}\left(\frac{1}{\Delta_l}+\frac{1}{\Delta_{l'}}\right)$, the first line of Eq. (9) describes Stark shifts while the second line represents the coupling between the qutrits l and l' induced by the cavity c.

If the auxiliary level $|f\rangle_l$ of qutrit l ($l=2,3,\cdots,N$) is not occupied, the effective Hamiltonian (9) reduces to

$$H_{e1}=-\sum_{l=2}^{N}\lambda_l\hat{a}_c^\dagger\hat{a}_c|e\rangle_l\langle e|. \tag{10}$$

Under the effective Hamiltonian (10), one can obtain the following state evolution

$$\begin{aligned}&|g\rangle_l|0\rangle_c\to|g\rangle_l|0\rangle_c,\quad &&|e\rangle_l|0\rangle_c\to|e\rangle_l|0\rangle_c,\\&|g\rangle_l|1\rangle_c\to|g\rangle_l|1\rangle_c,\quad &&|e\rangle_l|1\rangle_c\to e^{i\lambda_l t}|e\rangle_l|1\rangle_c.\end{aligned} \tag{11}$$

2.4 Cavity–cavity cross-Kerr interaction

Consider cavity c and cavity j ($j=1,2,3,\cdots,N$) are dispersively coupled to the qutrit q [Fig. 2(e)]. As shown in Fig. 2(e), cavity c (j) is dispersively coupled to the $|g\rangle_q\leftrightarrow|e\rangle_q$ ($|e\rangle_q\leftrightarrow|f\rangle_q$) transition of qutrit q with coupling strength μ_c (μ_j). In the interaction picture and after making the RWA, the Hamiltonian is given by

$$H_5=\mu_c(e^{i\delta_c t}\hat{a}_c\sigma_{eg,q}^{+}+h.c.)+\sum_{j=1}^{N}\mu_j(e^{i\delta_{c_j}t}\hat{a}_j\sigma_{fe,q}^{+}+h.c.), \tag{12}$$

where $\hat{a}_j$ is the photon annihilation operator of cavity j, $\sigma_{eg,q}^{+}=|e\rangle_q\langle g|$, $\sigma_{fe,q}^{+}=|f\rangle_q\langle e|$, $\delta_c=\omega_{eg,q}-\omega_c<0$ and $\delta_{c_j}=\omega_{fe,q}-\omega_{c_j}>0$. Here, $\omega_{fe,q}$ and $\omega_{eg,q}$ are the $|e\rangle_q\leftrightarrow|f\rangle_q$ and $|g\rangle_q\leftrightarrow|e\rangle_q$ transition frequencies of qutrit q, and ω_c and ω_{c_j} are the frequencies of cavities c and j ($j=1,2,3,\cdots,N$), respectively.

Under the large-detuning conditions $|\delta_c|\gg\mu_c$ and $\delta_{c_j}\gg\mu_j$, the Hamiltonian (12) becomes [71–73]

$$\begin{aligned}H_{e2}=&\lambda_c(\hat{a}_c^\dagger\hat{a}_c|g\rangle_q\langle g|-\hat{a}_c\hat{a}_c^\dagger|e\rangle_q\langle e|)\\&-\sum_{j=1}^{N}\frac{\mu_j^2}{\delta_{c_j}}(\hat{a}_j^\dagger\hat{a}_j|e\rangle_q\langle e|-\hat{a}_j\hat{a}_j^\dagger|f\rangle_q\langle f|)\\&+\sum_{j\neq j'=1}^{N}\lambda_{jj'}e^{i\delta_{jj'}t}\hat{a}_j\hat{a}_{j'}^\dagger(|f\rangle_q\langle f|-|e\rangle_q\langle e|)\\&+\sum_{j=1}^{N}\lambda_j(e^{-i\delta_j t}\hat{a}_c^\dagger\hat{a}_j^\dagger\sigma_{fg,q}^{-}+h.c.),\end{aligned} \tag{13}$$

where $\lambda_c=-\frac{\mu_c^2}{\delta_c}$, $\lambda_{jj'}=\frac{\mu_j\mu_{j'}}{2}(\frac{1}{\delta_{c_j}}+\frac{1}{\delta_{c_{j'}}})$, $\lambda_j=\frac{\mu_c\mu_j}{2}(\frac{1}{|\delta_c|}+\frac{1}{\delta_{c_j}})$, $\delta_{jj'}=\delta_{c_j}-\delta_{c_{j'}}$, $\delta_j=\omega_{fg,q}-\omega_c-\omega_{c_j}>0$, and $\sigma_{fg}^{-}=|g\rangle_q\langle f|$. Here, $\omega_{fg,q}$ is the $|f\rangle_q\leftrightarrow|g\rangle_q$ transition frequency of qutrit q.

Considering the large-detuning conditions $\delta_j\gg\{\lambda_c,\mu_j^2/\delta_j,\lambda_{jj'},\lambda_j\}$, the effective Hamiltonian (13) turns into [71–73]

$$\begin{aligned}H_{e2}=&\lambda_c(\hat{a}_c^\dagger\hat{a}_c|g\rangle_q\langle g|-\hat{a}_c\hat{a}_c^\dagger|e\rangle_q\langle e|)\\&-\sum_{j=1}^{N}\frac{\mu_j^2}{\delta_{c_j}}(\hat{a}_j^\dagger\hat{a}_j|e\rangle_q\langle e|-\hat{a}_j\hat{a}_j^\dagger|f\rangle_q\langle f|)\\&+\sum_{j\neq j'=1}^{N}\lambda_{jj'}e^{i\delta_{jj'}t}\hat{a}_j\hat{a}_{j'}^\dagger(|f\rangle_q\langle f|-|e\rangle_q\langle e|)\\&+\sum_{j=1}^{N}\chi_j(\hat{a}_c\hat{a}_c^\dagger\hat{a}_j\hat{a}_j^\dagger|f\rangle_q\langle f|-\hat{a}_c^\dagger\hat{a}_c\hat{a}_j^\dagger\hat{a}_j|g\rangle_q\langle g|),\end{aligned} \tag{14}$$

where $\chi_j=\lambda_j^2/\delta_j$ is the effective cross-Kerr interaction coupling strength between cavities c and j.

When the levels $|e\rangle_q$ and $|f\rangle_q$ of qutrit q are not occupied, the Hamiltonian (14) reduces to the effective Hamiltonian [71–73]

$$H_{e2}=\lambda_c\hat{n}_c|g\rangle_q\langle g|-\sum_{j=1}^{N}\chi_j\hat{n}_c\hat{n}_j|g\rangle_q\langle g|, \tag{15}$$

where $\hat{n}_c=\hat{a}_c^\dagger\hat{a}_c$ and $\hat{n}_j=\hat{a}_j^\dagger\hat{a}_j$ are the photon number operators for cavities c and j, respectively.

2.5 Cavity–qutrit-pulse dispersive interaction

Assume that cavity 1 and a microwave pulse are dispersively coupled to the $|g\rangle_q\leftrightarrow|e\rangle_q$ transition of qutrit q, respectively [Fig. 2(f)]. By applying the RWA, the Hamiltonian in the interaction picture is

$$H_6=g_q e^{i\delta_q t}\hat{a}_1\sigma_{eg,q}^{+}+\Omega_p e^{-i[(\omega_p-\omega_{eg,q})t+\phi_p]}\sigma_{eg,q}^{+}+h.c., \tag{16}$$

where g_q is the coupling strength, $\delta_q=\omega_{eg,q}-\omega_{c_1}>0$ is the detunings, Ω_p, ω_p, and ϕ_p are respectively the Rabi frequency, frequency, and initial phase of the pulse.

Under the large-detuning condition $\delta_q\gg g_q$ and assuming $\delta_q\gg\Omega_p$, one can obtain the effective Hamiltonian [71–73]

$$\begin{aligned}H_{e3}=&\lambda_q\left(\hat{a}_1^{+}\hat{a}_1+\frac{1}{2}\right)\sigma_{z,q}\\&+\Omega_p\left(e^{-i[(\omega_p-\omega_{eg,q})t+\phi_p]}\sigma_{eg,q}^{+}+h.c.\right),\end{aligned} \tag{17}$$

where $\lambda_q=\frac{g_q^2}{\delta_q}$ and $\sigma_{z,q}=|e\rangle_q\langle e|-|g\rangle_q\langle g|$. In a rotating frame under the Hamiltonian $\lambda_q\left(\hat{a}_1^{+}\hat{a}_1+\frac{1}{2}\right)\sigma_{z,q}$ and for $\omega_p=\omega_{eg,q}+\lambda_q$, one has

$$H_{e3}=\Omega_p e^{-i\phi_p}e^{-i2\lambda_q\hat{a}_1^{+}\hat{a}_1 t}\sigma_{eg,q}^{+}+h.c.. \tag{18}$$

We then discuss how to use Eq. (18) to realize the following state rotations depending on the initial state of cavity 1.

(i) If the cavity 1 is in the vacuum state $|0\rangle_{c_1}$, the Hamiltonian (18) reduces to $H_{e3}=\Omega_p e^{-i\phi_p}\sigma_{eg,q}^{+}+h.c.$. One can easily obtain the following rotations

$$\begin{aligned}|g\rangle_q|0\rangle_{c_1}&\rightarrow\left[\cos(\Omega_p t)|g\rangle_q-ie^{-i\phi_p}\sin(\Omega_p t)|e\rangle_q\right]|0\rangle_{c_1},\\ |e\rangle_q|0\rangle_{c_1}&\rightarrow\left[\cos(\Omega_p t)|e\rangle_q-ie^{i\phi_p}\sin(\Omega_p t)|g\rangle_q\right]|0\rangle_{c_1}.\end{aligned}\tag{19}$$

After returning to the original interaction picture by performing a unitary transformation $\exp\left\{-i\left[\lambda_q\left(\hat{a}_1^{+}\hat{a}_1+\frac{1}{2}\right)\sigma_{z,q}\right]t\right\}$, one has the following state transformations according to (19)

$$\begin{aligned}|g\rangle_q|0\rangle_{c_1}\rightarrow&\left[e^{i\frac{\lambda_q}{2}t}\cos(\Omega_p t)|g\rangle_q\right.\\&\left.-ie^{-i(\phi_p+\frac{\lambda_q}{2}t)}\sin(\Omega_p t)|e\rangle_q\right]|0\rangle_{c_1},\\ |e\rangle_q|0\rangle_{c_1}\rightarrow&\left[e^{-i\frac{\lambda_q}{2}t}\cos(\Omega_p t)|e\rangle_q\right.\\&\left.-ie^{i(\phi_p+\frac{\lambda_q}{2}t)}\sin(\Omega_p t)|g\rangle_q\right]|0\rangle_{c_1}.\end{aligned}\tag{20}$$

(ii) If the cavity 1 is in the coherent state $|2\alpha\rangle_{c_1}$, we assume that α is sufficiently large such that $2\lambda_q\overline{n}\gg\Omega_p$, where $\overline{n}=4|\alpha|^2$ is the average photon number of the coherent state $|2\alpha\rangle_{c_1}$. Thus, the states of qutrit q are not changed by the microwave pulse [74], i.e.,

$$|g\rangle_q|2\alpha\rangle_{c_1}\rightarrow|g\rangle_q|2\alpha\rangle_{c_1},\quad|e\rangle_q|2\alpha\rangle_{c_1}\rightarrow|e\rangle_q|2\alpha\rangle_{c_1}.\tag{21}$$

After returning to the original interaction picture by performing a unitary transformation $\exp\left\{-i\left[\lambda_q\left(\hat{a}_1^{+}\hat{a}_1+\frac{1}{2}\right)\sigma_{z,q}\right]t\right\}$, we have

$$\begin{aligned}|g\rangle_q|2\alpha\rangle_{c_1}&\rightarrow e^{i\frac{\lambda_q}{2}t}|g\rangle_q|2\alpha e^{i\lambda_q t}\rangle_{c_1},\\ |e\rangle_q|2\alpha\rangle_{c_1}&\rightarrow e^{-i\frac{\lambda_q}{2}t}|e\rangle_q|2\alpha e^{-i\lambda_q t}\rangle_{c_1}.\end{aligned}\tag{22}$$

The above results (3), (5), (7), (11), (15), (20), and (22) will be used to transfer quantum entangled states from a group of SC qubits to another group of MF qubits, as discussed in the next section.

3 Transfer of entangled states between SC qubits and MF qubits

Let us return to the setup illustrated in Fig. 1. Suppose that the superconducting qutrits $\{1,2,3,\cdots,N\}$ are initially prepared in a GHZ state $a|g\rangle_1|g\rangle_2\ldots|g\rangle_N+b|e\rangle_1|e\rangle_2\ldots|e\rangle_N$, the cavity c is initially in the vacuum state $|0\rangle_c$, the qutrit q is in the ground state $|g\rangle_q$, and each of cavities $\{1,2,3,\cdots,N\}$ is in a coherent state $|\alpha\rangle$. Thus, the initial state of the whole system can be written as

$$\begin{aligned}&(a|g\rangle_1|g\rangle_2\ldots|g\rangle_N+b|e\rangle_1|e\rangle_2\ldots|e\rangle_N)\\&\cdot|g\rangle_q|0\rangle_c|\alpha\rangle_{c_1}|\alpha\rangle_{c_2}\ldots|\alpha\rangle_{c_N},\end{aligned}\tag{23}$$

where subscripts $c_1,c_2,\cdots,c_N$ represent cavities $1,2,\cdots,$ and N, respectively. We suppose all qutrits, i.e., qutrits $(1,2,3,\cdots,N)$ and q, are initially decoupled from their respective cavities. Note that the qutrit-cavity coupling and decoupling can be achieved by prior adjustment of the level spacings of qutrits or prior adjustment of the frequencies of cavities. For superconducting qutrits and microwave cavities, the level spacings of qutrits and the frequencies of cavities can be rapidly adjusted within a few nanoseconds [4–6, 75, 76].

The procedure for transferring the entangled states from SC qubits to MF qubits is listed below.

Step 1. Apply a microwave pulse (with an initial phase $\phi_l=-\pi/2$) to qutrit l $(l=2,3,\cdots,N)$. The pulse is resonant with the $|g\rangle_l\leftrightarrow|e\rangle_l$ transition of qutrit l [Fig. 2(a)]. For a duration time $t_1=\pi/(4\Omega_l)$ and according to Eq. (3), one can obtain the state transformation $|g\rangle_l\rightarrow|+\rangle_l$ and $|e\rangle_l\rightarrow|-\rangle_l$ with $|+\rangle_l=(|e\rangle_l+|g\rangle_l)/\sqrt{2}$ and $|-\rangle_l=(|e\rangle_l-|g\rangle_l)/\sqrt{2}$. The state (23) thus becomes

$$\begin{aligned}&(a|g\rangle_1|+\rangle_2|+\rangle_3\ldots|+\rangle_N+b|e\rangle_1|-\rangle_2|-\rangle_3\ldots|-\rangle_N)\\&\cdot|g\rangle_q|0\rangle_c|\alpha\rangle_{c_1}|\alpha\rangle_{c_2}|\alpha\rangle_{c_3}\ldots|\alpha\rangle_{c_N}.\end{aligned}\tag{24}$$

Step 2. Adjust the frequency of qutrit 1 such that the $|g\rangle_1\leftrightarrow|e\rangle_1$ transition of qutrit 1 is resonant with cavity c [Fig. 2(b)]. The interaction Hamiltonian is given by Eq. (4). According to Eq. (5), one has $|e\rangle_1|0\rangle_c\rightarrow-i|g\rangle_1|1\rangle_c$ for an interaction time $t_2=\pi/(2g_{r,1})$. The state (24) then becomes

$$\begin{aligned}&|g\rangle_q|g\rangle_1(a|+\rangle_2|+\rangle_3\ldots|+\rangle_N|0\rangle_c-ib|-\rangle_2|-\rangle_3\\&\ldots|-\rangle_N|1\rangle_c)\otimes|\alpha\rangle_{c_1}|\alpha\rangle_{c_2}|\alpha\rangle_{c_3}\ldots|\alpha\rangle_{c_N}.\end{aligned}\tag{25}$$

After this step of operation, we adjust the level configuration of qutrit 1 and make the qutrit 1 decoupled from the cavity c.

Step 3. Adjust the frequency of qutrit l $(l=2,3,\cdots,N)$ such that the $|e\rangle_l\leftrightarrow|f\rangle_l$ transition of qutrit l is dispersively coupled to cavity c [Fig. 2(d)]. The effective Hamiltonian and state evolution of this operation have been given by Eqs. (10) and (11), respectively. According to Eq. (11), one has $|g\rangle_l|1\rangle_c\rightarrow|g\rangle_l|1\rangle_c$ and $|e\rangle_l|1\rangle_c\rightarrow-|e\rangle_l|1\rangle_c$ (i.e., $|-\rangle_l|1\rangle_c\rightarrow-|+\rangle_l|1\rangle_c$) for an operational time $t_3=\pi/\lambda_l$ $(l=2,3,\cdots,N)$. Thus, the state (25) changes to

$$\begin{aligned}&|g\rangle_q|g\rangle_1|+\rangle_2|+\rangle_3\ldots|+\rangle_N\left[a|0\rangle_c-(-1)^{N-1}ib|1\rangle_c\right]\\&\otimes|\alpha\rangle_{c_1}|\alpha\rangle_{c_2}|\alpha\rangle_{c_3}\ldots|\alpha\rangle_{c_N}.\end{aligned}\tag{26}$$

After this step of operation, we adjust the level configuration of qutrit l $(l=2,3,\cdots,N)$ such that the qutrit

l is decoupled from the cavity c. Here, we have set $\lambda_2 = \lambda_3 = \cdots = \lambda_N$.

Step 4. Adjust the frequency of qutrit q such that the cavities c and j ($j = 1, 2, 3, \cdots, N$) are dispersively coupled to the $|g\rangle_q \leftrightarrow |e\rangle_q$ and $|e\rangle_q \leftrightarrow |f\rangle_q$ transitions of qutrit q, respectively [Fig. 2(e)]. The effective Hamiltonian of this subsystem has been derived in Eq. (15). Under the Hamiltonian (15), the state (26) evolves into

$$\begin{aligned}&|g\rangle_q|g\rangle_1|+\rangle_2|+\rangle_3\ldots|+\rangle_N\left[a|0\rangle_c|\alpha\rangle_{c_1}|\alpha\rangle_{c_2}|\alpha\rangle_{c_3}\ldots|\alpha\rangle_{c_N}\right.\\&-(-1)^{N-1}\mathrm{i}b\mathrm{e}^{-\mathrm{i}\lambda_c t_4}|1\rangle_c\\&\left.\otimes|\alpha\mathrm{e}^{\mathrm{i}\chi_1 t_4}\rangle_{c_1}|\alpha\mathrm{e}^{\mathrm{i}\chi_2 t_4}\rangle_{c_2}|\alpha\mathrm{e}^{\mathrm{i}\chi_3 t_4}\rangle_{c_3}\ldots|\alpha\mathrm{e}^{\mathrm{i}\chi_N t_4}\rangle_{c_N}\right].\end{aligned}\tag{27}$$

For an evolution time $t_4 = \pi/\chi_j$ ($j = 1, 2, 3, \cdots, N$), the state (27) turns into

$$\begin{aligned}&|g\rangle_q|g\rangle_1|+\rangle_2|+\rangle_3\ldots|+\rangle_N\left(a|0\rangle_c|\alpha\rangle_{c_1}|\alpha\rangle_{c_2}|\alpha\rangle_{c_3}\ldots|\alpha\rangle_{c_N}\right.\\&\left.-(-1)^{N-1}\mathrm{i}b\mathrm{e}^{-\mathrm{i}\varphi}|1\rangle_c|-\alpha\rangle_{c_1}|-\alpha\rangle_{c_2}|-\alpha\rangle_{c_3}\ldots|-\alpha\rangle_{c_N}\right)\end{aligned}\tag{28}$$

with $\varphi = \lambda_c\pi/\chi_j$ ($j = 1, 2, 3, \cdots, N$). After completing this operation, the level configuration of qutrit q should be adjusted such that the qutrit q is decoupled from cavity c and j ($j = 1, 2, 3, \cdots, N$). Here, we have assumed $\chi_1 = \chi_2 = \cdots = \chi_N$.

Step 5. Adjust the frequency of qutrit q such that the $|g\rangle_q \leftrightarrow |e\rangle_q$ transition of qutrit q is resonant with cavity c [Fig. 2(c)]. According to Eq. (7), one has $|g\rangle_q|1\rangle_c \to \mathrm{i}|e\rangle_q|0\rangle_c$ for interaction time $t_5 = 3\pi/(2g_{r,q})$. The state (28) then becomes

$$\begin{aligned}&|g\rangle_1|+\rangle_2|+\rangle_3\ldots|+\rangle_N|0\rangle_c\left(a|g\rangle_q|\alpha\rangle_{c_1}|\alpha\rangle_{c_2}|\alpha\rangle_{c_3}\ldots|\alpha\rangle_{c_N}\right.\\&\left.+(-1)^{N-1}b\mathrm{e}^{-\mathrm{i}\varphi}|e\rangle_q|-\alpha\rangle_{c_1}|-\alpha\rangle_{c_2}|-\alpha\rangle_{c_3}\ldots|-\alpha\rangle_{c_N}\right).\end{aligned}\tag{29}$$

After this operation, one adjusts the level configuration of qutrit q such that the qutrit q is decoupled from the cavity c. Apply the displacement operator $\hat{D}(\alpha)$ to cavity 1 such that $|\alpha\rangle_{c_1} \to |2\alpha\rangle_{c_1}$ and $|-\alpha\rangle_{c_1} \to |0\rangle_{c_1}$, the state (29) thus becomes

$$\begin{aligned}&|g\rangle_1|+\rangle_2|+\rangle_3\ldots|+\rangle_N|0\rangle_c\left(a|g\rangle_q|2\alpha\rangle_{c_1}|\alpha\rangle_{c_2}|\alpha\rangle_{c_3}\ldots|\alpha\rangle_{c_N}\right.\\&\left.+(-1)^{N-1}b\mathrm{e}^{-\mathrm{i}\varphi}|e\rangle_q|0\rangle_{c_1}|-\alpha\rangle_{c_2}|-\alpha\rangle_{c_3}\ldots|-\alpha\rangle_{c_N}\right).\end{aligned}\tag{30}$$

Step 6. Adjust the frequency of qutrit q such that the $|g\rangle_q \leftrightarrow |e\rangle_q$ transition of qutrit q is dispersively coupled to cavity 1 and a microwave pulse, respectively [Fig. 2(f)]. According to Eqs. (20) and (22), we have $|e\rangle_q|0\rangle_{c_1} \to -\mathrm{i}\mathrm{e}^{\mathrm{i}(\phi_p+\frac{\lambda_q}{2}t_6)}|g\rangle_q|0\rangle_{c_1}$ and $|g\rangle_q|2\alpha\rangle_{c_1} \to \mathrm{e}^{\mathrm{i}\frac{\lambda_q}{2}t_6}|g\rangle_q|2\alpha\mathrm{e}^{\mathrm{i}\lambda_q t_6}\rangle_{c_1}$ for an interaction time $t_6 = \pi/(2\Omega_p)$. The state (30) then turns into

$$\begin{aligned}&|g\rangle_q|g\rangle_1|+\rangle_2|+\rangle_3\ldots|+\rangle_N|0\rangle_c\left(a|2\alpha\rangle_{c_1}|\alpha\rangle_{c_2}|\alpha\rangle_{c_3}\ldots|\alpha\rangle_{c_N}\right.\\&\left.+b|0\rangle_{c_1}|-\alpha\rangle_{c_2}|-\alpha\rangle_{c_3}\ldots|-\alpha\rangle_{c_N}\right),\end{aligned}\tag{31}$$

where we have set $\phi_p - \varphi = \pm\pi/2$ and $\lambda_q t_6 = 2\pi$, and a common phase factor $\mathrm{e}^{\mathrm{i}\pi}$ is dropped off. Here, $\phi_p - \varphi = \pi/2$ for an odd N, while $\phi_p - \varphi = -\pi/2$ for an even N. Then, adjust the level configuration of qutrit q so that the qutrit q is decoupled from cavity 1. Finally, apply the displacement operator $\hat{D}(-\alpha)$ to cavity 1 such that $|2\alpha\rangle_{c_1} \to |\alpha\rangle_{c_1}$ and $|0\rangle_{c_1} \to |-\alpha\rangle_{c_1}$. The state (31) thus becomes

$$\begin{aligned}&|g\rangle_q|g\rangle_1|+\rangle_2|+\rangle_3\ldots|+\rangle_N|0\rangle_c\left(a|\alpha\rangle_{c_1}|\alpha\rangle_{c_2}|\alpha\rangle_{c_3}\ldots|\alpha\rangle_{c_N}\right.\\&\left.+b|-\alpha\rangle_{c_1}|-\alpha\rangle_{c_2}|-\alpha\rangle_{c_3}\ldots|-\alpha\rangle_{c_N}\right),\end{aligned}\tag{32}$$

which shows that the quantum entangled state of N SC qubits has been transferred onto N MF qubits.

As described in the above steps, the cavity–qutrit coupling or decoupling is achieved by adjusting the level spacings of the qutrits. Because the rapid tuning of cavity frequencies has been reported in experiments [75, 76], one can also tune the frequencies of cavities such that the cavities are coupled to or decoupled from the qutrits.

Before ending this section, several points need to be addressed as follows:

(i) In Step 3 above, we have set $\lambda_2 = \lambda_3 = \cdots = \lambda_N$, i.e.,

$$\frac{g_2^2}{\Delta_2} = \frac{g_3^2}{\Delta_3} = \cdots = \frac{g_N^2}{\Delta_N}.\tag{33}$$

Because of $\Delta_l = \omega_{fe,l} - \omega_c$ ($l = 2, 3, \cdots, N$), the condition (33) can be met by carefully selecting the detunings Δ_2, Δ_3, $\cdots$, Δ_N via adjusting the level spacing of qutrits $(2, 3, \cdots, N)$.

(ii) In Step 4 above, we have assumed $\chi_1 = \chi_2 = \cdots = \chi_{N-1} = \chi_N$. This condition can be further written as

$$\frac{\mu_1(|\delta_c| + \delta_{c_1})}{\sqrt{\delta_1}\delta_{c_1}} = \frac{\mu_2(|\delta_c| + \delta_{c_2})}{\sqrt{\delta_2}\delta_{c_2}} = \cdots = \frac{\mu_N(|\delta_c| + \delta_{c_N})}{\sqrt{\delta_N}\delta_{c_N}},\tag{34}$$

which can be satisfied by selecting the detunings δ_{c_j}, δ_j ($j = 1, 2, \cdots, N$), and δ_c through adjusting the level spacing of qutrits or tuning the frequencies of cavity c and cavity j ($j = 1, 2, \cdots, N$).

(iii) In Step 6 above, we have set $t_6 = \pi/(2\Omega_p)$ and $\lambda_q t_6 = 2\pi$, resulting in $\frac{2\pi}{\lambda_q} = \frac{\pi}{2\Omega_p}$. This condition can be further expressed as

$$\Omega_p = \frac{g_q^2}{4\delta_q},\tag{35}$$

which can be easily met by adjusting the Rabi frequency Ω_p of the driving pulse.

(iv) Since no measurement is used in the above, all operations involved in the state transfer are unitary operations. Thus, the entangled states can be transferred back from the MF qubits to the SC qubits by performing reverse operations.

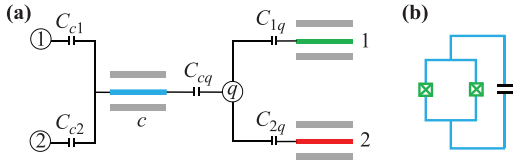

Fig. 3 **(a)** Diagram of setup consisting of three 1D superconducting resonators (1, 2, c) and three superconducting transmon qutrits (1, 2, q), in which resonator c is capacitively coupled to transmon qutrits (1, 2, q) via capacitances (C_{c1}, C_{c2}, C_{cq}), and transmon qutrit q is capacitively coupled to resonators (1, 2) via capacitances (C_{1q}, C_{2q}). **(b)** Circuit diagram of a transmon qutrit, which consists of two Josephson junctions and a capacitor.

4 Possible experimental implementation

In this section, as an example, we investigate the experimental feasibility for transferring entangled states from two SC qubits (1, 2) to two MF qubits (1, 2) [i.e., converting the initial state (23) into the target state (32) with $N = 2$], by a setup consisting of three one-dimensional (1D) superconducting resonators (1, 2, c) and three superconducting transmon qutrits (1, 2, q) (Fig. 3). In Steps 5 and 6, we have used the displacement operators $\hat{D}(\alpha)$ and $\hat{D}(-\alpha)$. The displacement operators $\hat{D}(\alpha)$ and $\hat{D}(-\alpha)$ are given by $\hat{D}(\alpha) = e^{\alpha\hat{a}^{\dagger}_{c_1} - \alpha^{*}\hat{a}_{c_1}}$ and $\hat{D}(-\alpha) = e^{\alpha^{*}\hat{a}_{c_1} - \alpha\hat{a}^{\dagger}_{c_1}}$ [77]. For the realization of the displacement operators $\hat{D}(\alpha)$ and $\hat{D}(-\alpha)$ in experiments, one can use a microwave pulse to drive the cavity 1 [78]. The corresponding Hamiltonian can be expressed as $\Omega(e^{i\phi_1}\hat{a}_{c_1} + e^{-i\phi_1}\hat{a}^{\dagger}_{c_1})$. One can choose a phase $\phi_1 = -\pi/2$ or $\phi_1 = \pi/2$ depending on the displacement operator $\hat{D}(\alpha)$ or $\hat{D}(-\alpha)$. Accordingly, we have $\alpha = \Omega t$. For a transmon qutrit, the $|g\rangle \leftrightarrow |f\rangle$ transition is forbidden or very weak [79]. Thus, the couplings of the cavity/pulse with the $|g\rangle \leftrightarrow |f\rangle$ transition can be neglected. Hereafter, the terms cavity and resonator are used interchangeably.

From the previous Section 3, one can see that six basic interactions are used in the transfer of entangled states, i.e., the six basic interactions described by the Hamiltonians H_1, H_2, H_3, H_4, H_5, and H_6 above. When the inter-cavity crosstalk and the unwanted interactions are considered, these Hamiltonians are modified as follows.

(i) $H_1' = H_1 + \delta H_1$ where δH_1 describes the unwanted interaction between the pulse and the $|e\rangle_l \leftrightarrow |f\rangle_l$ transition of qutrit l ($l = 2$) [Fig. 4(a)]. The Hamiltonian δH_1 is given by

$$\delta H_1 = \widetilde{\Omega}_l \left(e^{-i\phi_l} e^{-i\Delta_{p,l}} \sigma^{+}_{fe,l} + h.c. \right), \tag{36}$$

where $\sigma^{+}_{fe,l} = |f\rangle_l\langle e|$, $\widetilde{\Omega}_l$ is the pulse Rabi frequency associated with the $|e\rangle_l \leftrightarrow |f\rangle_l$ transition of the qutrit l, and $\Delta_{p,l} = \omega_p' - \omega_{fe,l} = \omega_{eg,l} - \omega_{fe,l} > 0$ is the detuning between the pulse frequency ω_p' and the $|e\rangle_l \leftrightarrow |f\rangle_l$ transition frequency of the qutrit l.

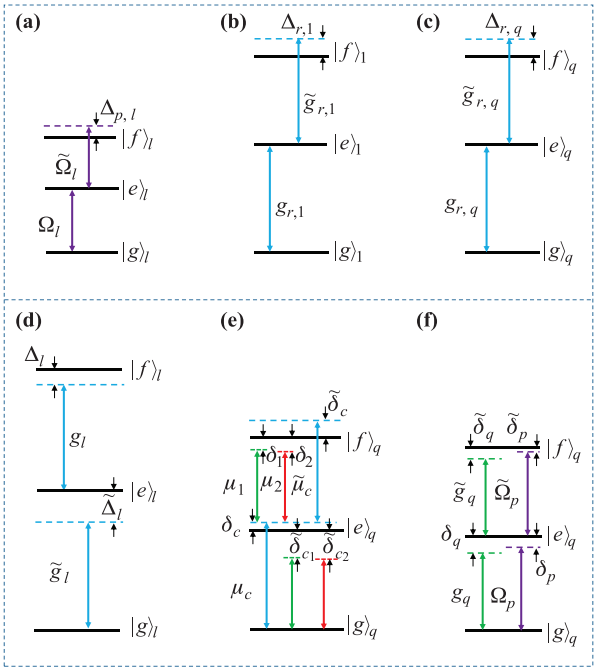

Fig. 4 **(a)** A microwave pulse resonant with the $|g\rangle_l \leftrightarrow |e\rangle_l$ transition of qutrit l ($l = 2$) with Rabi frequency Ω_l, while far-off resonant with the $|e\rangle_l \leftrightarrow |f\rangle_l$ transition of qutrit l with Rabi frequency $\widetilde{\Omega}_l$ and detuning $\Delta_{p,l}$. **(b)** Cavity c resonant with the $|g\rangle_1 \leftrightarrow |e\rangle_1$ transition of qutrit 1 with coupling strength $g_{r,1}$, while far-off resonant with the $|e\rangle_1 \leftrightarrow |f\rangle_1$ transition of qutrit 1 with coupling strength $\widetilde{g}_{r,1}$ and detuning $\Delta_{r,1} > 0$. **(c)** Cavity c resonant with the $|g\rangle_q \leftrightarrow |e\rangle_q$ transition of qutrit q with coupling strength $g_{r,q}$, while far-off resonant with the $|e\rangle_q \leftrightarrow |f\rangle_q$ transition of qutrit q with coupling strength $\widetilde{g}_{r,q}$ and detuning $\Delta_{r,q} > 0$. **(d)** Cavity c dispersively coupled to the $|e\rangle_l \leftrightarrow |f\rangle_l$ ($|g\rangle_l \leftrightarrow |e\rangle_l$) transition of qutrit l ($l = 2$) with coupling strength g_l ($\widetilde{g}_l$) and detuning Δ_l ($\widetilde{\Delta}_l$). **(e)** Cavity c dispersively coupled to $|g\rangle_q \leftrightarrow |e\rangle_q$ ($|e\rangle_q \leftrightarrow |f\rangle_q$) transition of qutrit q with coupling strength μ_c ($\widetilde{\mu}_c$) and detuning $\delta_c < 0$ ($\widetilde{\delta}_c < 0$), while cavity j ($j = 1, 2$) is dispersively coupled to $|e\rangle_q \leftrightarrow |f\rangle_q$ ($|g\rangle_q \leftrightarrow |e\rangle_q$) transition of qutrit q with coupling strength μ_j ($\widetilde{\mu}_j$) and detuning $\delta_{c_j} > 0$ ($\widetilde{\delta}_{c_j} > 0$). **(f)** Cavity 1 and a microwave pulse dispersively coupled to the $|g\rangle_q \leftrightarrow |e\rangle_q$ ($|e\rangle_q \leftrightarrow |f\rangle_q$) transition of qutrit q. Here, g_q and $\widetilde{g}_q$ are the coupling strengths, δ_q and $\widetilde{\delta}_q$ are the detunings, Ω_p and $\widetilde{\Omega}_p$ are the pluse Rabi frequencies, δ_p and $\widetilde{\delta}_p = \omega_{fe,q} - \omega_p$ are the detunings.

(ii) $H_2' = H_2 + \delta H_2$, $H_3' = H_3 + \delta H_3$, where δH_2 describes the unwanted interaction between cavity c and the $|e\rangle_1 \leftrightarrow |f\rangle_1$ transition of qutrit 1 [Fig. 4(b)], while δH_3 describes the unwanted interaction between cavity c and the $|e\rangle_q \leftrightarrow |f\rangle_q$ transition of qutrit q [Fig. 4(c)]. The expression of Hamiltonians δH_2 and δH_3 are given by

$$\begin{aligned} \delta H_2 &= \tilde{g}_{r,1} \left(e^{-i\Delta_{r,1}t} \hat{a}_c \sigma^{+}_{fe,1} + h.c. \right), \\ \delta H_3 &= \tilde{g}_{r,q} \left(e^{-i\Delta_{r,q}t} \hat{a}_c \sigma^{+}_{fe,q} + h.c. \right), \end{aligned} \tag{37}$$

where $\sigma^{+}_{fe,1} = |f\rangle_1\langle e|$, $\sigma^{+}_{fe,q} = |f\rangle_q\langle e|$, $\tilde{g}_{r,1}$ ($\tilde{g}_{r,q}$) is the

off-resonant coupling strength between cavity c and the $|e\rangle_1 \leftrightarrow |f\rangle_1$ ($|e\rangle_q \leftrightarrow |f\rangle_q$) transition of qutrit 1 (q), and $\Delta_{r,1} = \omega_c - \omega_{fe,1} = \omega_{eg,1} - \omega_{fe,1} > 0$ ($\Delta_{r,q} = \omega_c - \omega_{fe,q} = \omega_{eg,q} - \omega_{fe,q} > 0$) is the detuning between the frequency of cavity c and the $|e\rangle_1 \leftrightarrow |f\rangle_1$ ($|e\rangle_q \leftrightarrow |f\rangle_q$) transition frequency of qutrit 1 (q).

(iii) $H_4' = H_4 + \delta H_4$ where δH_4 describes the unwanted interaction of cavity c with the $|g\rangle_l \leftrightarrow |e\rangle_l$ transition of the qutrit l ($l = 2$) [Fig. 4(d)]. The Hamiltonian δH_4 is given by

$$\delta H_4 = \widetilde{g}_l \left(\mathrm{e}^{\mathrm{i}\widetilde{\Delta}_l t} \hat{a}_c \sigma_{eg,l}^{+} + h.c. \right), \tag{38}$$

where $\widetilde{g}_l$ is the coupling strength between cavity c and the $|g\rangle_l \leftrightarrow |e\rangle_l$ transition of qutrit l and $\widetilde{\Delta}_l = \omega_{eg,l} - \omega_c = \omega_{eg,l} - \omega_{fe,l} + \Delta_l$ is the detuning between the frequency of cavity c and the $|g\rangle_l \leftrightarrow |e\rangle_l$ transition frequency of qutrit l.

(iv) $H_5' = H_5 + \delta H_5 + \varepsilon$, where δH_5 describes the unwanted coupling between cavity c and the $|e\rangle_q \leftrightarrow |f\rangle_q$ transition of qutrit q as well as the unwanted coupling between cavity j ($j = 1,\ 2$) and the $|g\rangle_q \leftrightarrow |e\rangle_q$ transition of qutrit q [Fig. 4(e)]. In addition, ε describes the intercavity crosstalk. The expression of δH_5 and ε are given by

$$\begin{aligned} \delta H_5 = {} & \widetilde{\mu}_c \left(\mathrm{e}^{\mathrm{i}\tilde{\delta}_c t} \hat{a}_c \sigma_{fe,q}^{+} + h.c. \right) \\ & + \sum_{j=1}^{2} \tilde{\mu}_j \left(\mathrm{e}^{\mathrm{i}\tilde{\delta}_{c_j} t} \hat{a}_j \sigma_{eg,q}^{+} + h.c. \right), \end{aligned} \tag{39}$$

$$\begin{aligned} \varepsilon = {} & \sum_{j=1}^{2} \mu_{cj} \left(\mathrm{e}^{-\mathrm{i}\widetilde{\Delta}_{cj} t} \hat{a}_c \hat{a}_j^{\dagger} + h.c. \right) \\ & + \mu_{12} \left(\mathrm{e}^{-\mathrm{i}\widetilde{\Delta}_{12} t} \hat{a}_1 \hat{a}_2^{\dagger} + h.c. \right), \end{aligned} \tag{40}$$

where $\widetilde{\mu}_c$ ($\widetilde{\mu}_j$) is the coupling strength between cavity c (j) and the $|e\rangle_q \leftrightarrow |f\rangle_q$ ($|g\rangle_q \leftrightarrow |e\rangle_q$) transition of qutrit q, $\tilde{\delta}_c = \omega_{fe,q} - \omega_c = \omega_{fe,q} - \omega_{eg,q} + \delta_c$ and $\widetilde{\delta}_{c_j} = \omega_{eg,q} - \omega_{c_j} = \omega_{eg,q} - \omega_{fe,q} + \delta_{c_j}$ ($j = 1,\ 2$) are detunings. μ_{cj} (μ_{12}) is the coupling strength between cavities c and j (1 and 2), $\widetilde{\Delta}_{cj} = \omega_c - \omega_{c_j}$ and $\widetilde{\Delta}_{12} = \omega_{c_1} - \omega_{c_2} = \delta_{c_2} - \delta_{c_1}$ are detunings.

(v) $H_6' = H_6 + \delta H_6$, where δH_6 represents the unwanted coupling between cavity 1 and the $|e\rangle_q \leftrightarrow |f\rangle_q$ transition of qutrit q as well as the unwanted interaction between the pulse and the $|e\rangle_q \leftrightarrow |f\rangle_q$ transition of qutrit q [Fig. 4(f)]. The expression of δH_6 is given by

$$\delta H_6 = \widetilde{g}_q \mathrm{e}^{\mathrm{i}\tilde{\delta}_q t} \hat{a}_1 \sigma_{fe,q}^{+} + \widetilde{\Omega}_p \mathrm{e}^{-\mathrm{i}[(\omega_p - \omega_{fe,q})t + \phi_p]} \sigma_{fe,q}^{+} + h.c., \tag{41}$$

where $\widetilde{g}_q$ is the coupling strength between cavity 1 and the $|e\rangle_q \leftrightarrow |f\rangle_q$ transition of qutrit q, $\widetilde{\Omega}_p$ is the Rabi frequency of the pulse (associated the $|e\rangle_q \leftrightarrow |f\rangle_q$ transition of qutrit q), and $\tilde{\delta}_q = \omega_{fe,q} - \omega_{c_1} = \omega_{fe,q} - \omega_{eg,q} + \delta_q$ is the detuning.

After taking into account the qutrit decoherence and the cavity decay, the dynamics of the lossy system is determined by the Markovian master equation

$$\begin{aligned} \frac{\mathrm{d}\rho}{\mathrm{d}t} = {} & -\mathrm{i}\left[H_k', \rho\right] + \sum_{l=1,2,c} \kappa_l \mathcal{L}\left[\hat{a}_l\right] \\ & + \sum_{j=1,2,q} \left(\gamma_{fe,j} \mathcal{L}\left[\sigma_{fe,j}^{-}\right] + \gamma_{fg,j} \mathcal{L}\left[\sigma_{fg,j}^{-}\right] \right. \\ & \left. + \gamma_{eg,j} \mathcal{L}\left[\sigma_{eg,j}^{-}\right] \right) \\ & + \sum_{j=1,2,q} \left(\gamma_{\varphi e,j} \mathcal{L}\left[\sigma_{ee,j}\right] + \gamma_{\varphi f,j} \mathcal{L}\left[\sigma_{ff,j}\right] \right), \end{aligned} \tag{42}$$

where ρ is the density matrix of system, H_k' (with $k = 1,\ 2,\ 3,\ 4,\ 5,\ 6$) are the modified Hamiltonians given above, $\mathcal{L}[\Lambda] = \Lambda\rho\Lambda^{+} - \Lambda^{+}\Lambda\rho/2 - \rho\Lambda^{+}\Lambda/2$, $\sigma_{fe,j}^{-} = |e\rangle_j\langle f|$, $\sigma_{fg,j}^{-} = |g\rangle_j\langle f|$, $\sigma_{eg,j}^{-} = |g\rangle_j\langle e|$, $\sigma_{ee,j} = |e\rangle_j\langle e|$, and $\sigma_{ff,j} = |f\rangle_j\langle f|$ ($j = 1,\ 2,\ q$). In addition, κ_l is the decay rate of the cavity l ($l = 1,\ 2,\ c$). $\gamma_{eg,j}$ is the energy relaxation rate of the state $|e\rangle$ for qutrit j, $\gamma_{fe,j}$ and $\gamma_{fg,j}$ are respectively the energy relaxation rates of the state $|f\rangle$ of qutrit j for the decay paths $|f\rangle \to |e\rangle$ and $|f\rangle \to |g\rangle$, $\gamma_{\varphi e,j}$ and $\gamma_{\varphi f,j}$ are the dephasing rates of the levels $|e\rangle_j$ and $|f\rangle_j$ of qutrit j, respectively.

The fidelity of the operation can be evaluated by $\mathcal{F} = \sqrt{\langle\psi_{\mathrm{id}}|\,\rho\,|\psi_{\mathrm{id}}\rangle}$, where $|\psi_{\mathrm{id}}\rangle$ is the ideal target state given by $|g\rangle_q|g\rangle_1|+\rangle_2|0\rangle_c\,(a|\alpha\rangle_{c_1}|\alpha\rangle_{c_2} + b|-\alpha\rangle_{c_1}|-\alpha\rangle_{c_2})$ with $N = 2$ according to Eq. (32). In addition, the initial state of the whole systems is given by $(a|g\rangle_1|g\rangle_2 + b|e\rangle_1|e\rangle_2)|g\rangle_q|0\rangle_c|\alpha\rangle_{c_1}|\alpha\rangle_{c_2}$ according to Eq. (23).

Typically, a transmon qutrit has small anharmonicity, but the recent experimental results show that the anharmonicity can be made to be $\sim$ 720 MHz [80]. Accordingly, the transmon anharmonicity is chosen by 700 MHz in our numerical simulation. As an example, consider $\Delta_{p,l}/(2\pi) = \Delta_{r,1}/(2\pi) = \Delta_{r,q}/(2\pi) = 0.7$ GHz. In addition, we choose $g_{r,1}/(2\pi) = g_{r,q}/(2\pi) = g_l/(2\pi) = g_q/(2\pi) = 50$ MHz, $\mu_c/(2\pi) = 100$ MHz, $\mu_1/(2\pi) = 76$ MHz, $\Omega_l/(2\pi) = 60$ MHz, $\Delta_l/(2\pi) = \delta_q/(2\pi) = 500$ MHz, $\delta_c/(2\pi) = -500$ MHz, $\delta_{c_1}/(2\pi) = 620$ MHz, $\delta_{c_2}/(2\pi) = 570$ MHz. According to Eq. (35), one has $\Omega_p/(2\pi) = 1.25$ MHz. For the parameters chosen here, we have $\varphi \approx 2\pi$ according to $\varphi = \lambda_c\pi/\chi_1$. Accordingly, we set $\phi_p \approx 1.5\pi$ for $\phi_p - \varphi = -\pi/2$. For the detunings $\{\delta_c,\ \delta_{c_1},\ \delta_{c_2}\}$ and the coupling constant μ_1 chosen here, we have $\mu_2/(2\pi) \approx 56$ MHz according to Eq. (34). The coupling strengths here are available in experiments [81]. For transmon qutrits [79], one has $\widetilde{g}_{r,1} = \sqrt{2}g_{r,1}$, $\widetilde{g}_{r,q} = \sqrt{2}g_{r,q}$, $\widetilde{g}_l = (1/\sqrt{2})g_l$, $\widetilde{\Omega}_l = \sqrt{2}\Omega_l$, $\widetilde{\mu}_c = \sqrt{2}\mu_c$, $\widetilde{\mu}_1 = (1/\sqrt{2})\mu_1$, $\widetilde{\mu}_2 = (1/\sqrt{2})\mu_2$, $\widetilde{\Omega}_p = \sqrt{2}\Omega_p$, and $\widetilde{g}_q = \sqrt{2}g_q$. In addition, we choose $\mu_{c1},\ \mu_{c2},\ \mu_{12} = 0.1\ \max\{\mu_c, \mu_1, \mu_2\}$ [42, 82]. Other parameters used in the numerical simulation are (i) $\gamma_{eg,j}^{-1} = 3T, \gamma_{fg,j}^{-1} = 10T$,

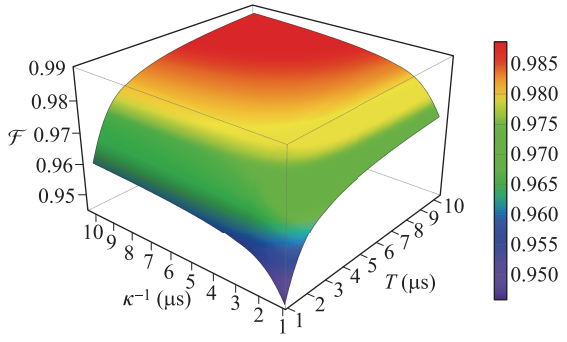

Fig. 5 Fidelity $\mathcal{F}$ versus κ^{-1} and T. The values of the parameters used here are given in the main text.

$\gamma_{fe,j}^{-1} = 1.5T, \gamma_{\varphi e,j}^{-1} = \gamma_{\varphi f,j}^{-1} = T$ $(j = 1, 2, q)$, (ii) $\kappa_l^{-1} = \kappa^{-1}$ $(l = 1, 2, c)$, (iii) $a = b = 1/\sqrt{2}$, (iv) $\alpha = 3.5$.

We plot Fig. 5 illustrating the fidelity versus T and κ^{-1} by numerically solving the master equation (42). Figure 5 displays that when $T \geqslant 4$ μs and $\kappa^{-1} \geqslant 3$ μs, the fidelity exceeds 98.0%. For $T =$ 4 μs, the decoherence times of the transmon qutrits are 4–40 μs, which is a rather conservative case because the decoherence time 55–300 μs for the transmon qutrit has been experimentally demonstrated [83, 84]. The entire operation time is ~ 0.63 μs, which is much shorter than the decoherence times of transmon qutrits used in our numerical simulations.

The frequency of a superconducting cavity is within a range of 1–15 GHz [5]. Thus, we choose $\omega_c/(2\pi) = 5.8$ GHz. According to the cavity-transmon detunings chosen above, one has the frequencies of cavities $\omega_{c_1}/(2\pi) = 3.98$ GHz and $\omega_{c_2}/(2\pi) = 4.03$ GHz. For the decay time of cavities $\kappa^{-1} = 3$ μs, the quality factors of the three cavities are $Q_c \sim 1.09\times10^5$, $Q_1 \sim 7.50\times10^4$, and $Q_2 \sim 7.59\times10^4$, which are available because 1D superconducting resonators with quality factors $> 10^6$ have been experimentally demonstrated [85, 86]. The above results show that the high-fidelity transfer of the entangled state from two SC qubits to two MF qubits can be achieved by utilizing current circuit QED technology.

5 Conclusion

We have proposed an approach to transfer an entangled state from a group of superconducting qubits to another group of microwave-field qubits. As shown above, only a coupler qutrit and auxiliary cavity are needed, thus the circuit architecture is simple. By using this proposal, the discrete-variable entangled state of superconducting qubits can be converted into the continuous-variable entangled coherent state of microwave-field qubits. Due to the third level $|f\rangle$ of each qutrit being not populated during the entire operation, the decoherence from qutrits' higher energy levels is greatly suppressed. Moreover, the entire operation time does not depend on the number of qubits, and the entangled state is deterministically transferred since no measurement is used. Numerical simulation shows that the entangled state of two superconducting qubits can be high-fidelity transferred to two microwave-field qubits within current circuit QED technology. Our proposal is quite general and can be applied to transfer entangled states between other matter qubits and microwave- or optical-field qubits encoded with coherent states.

Acknowledgements This work was partly supported by the Key-Area Research and Development Program of Guang Dong Province (Grant No. 2018B030326001), the National Natural Science Foundation of China (NSFC) (Grant Nos. 12004253, 11074062, 11374083, 11774076, 11804228, 11965017, and U21A20436), and the Jiangxi Natural Science Foundation (Grant Nos. 20192ACBL20051, 20212BAB211019, and 20212BAB201025).

References

1. C. P. Yang, S. I. Chu, and S. Han, Possible realization of entanglement, logical gates, and quantum information transfer with superconducting-quantum-interference-device qubits in cavity QED, *Phys. Rev. A* 67(4), 042311 (2003)
2. J. Q. You and F. Nori, Quantum information processing with superconducting qubits in a microwave field, *Phys. Rev. B* 68(6), 064509 (2003)
3. A. Blais, R. S. Huang, A. Wallraff, S. M. Girvin, and R. J. Schoelkopf, Cavity quantum electrodynamics for superconducting electrical circuits: An architecture for quantum computation, *Phys. Rev. A* 69(6), 062320 (2004)
4. J. Q. You and F. Nori, Atomic physics and quantum optics using superconducting circuits, *Nature* 474(7353), 589 (2011)
5. S. Schmidt and J. Koch, Circuit QED lattices: Towards quantum simulation with superconducting circuits, *Ann. Phys.* 525(6), 395 (2013)
6. X. Gu, A. F. Kockum, A. Miranowicz, Y. X. Liu, and F. Nori, Microwave photonics with superconducting quantum circuits, *Phys. Rep.* 718–719, 1 (2017)
7. T. Niemczyk, F. Deppe, H. Huebl, E. P. Menzel, F. Hocke, M. J. Schwarz, J. J. Garcia-Ripoll, D. Zueco, T. Hümmer, E. Solano, A. Marx, and R. Gross, Circuit quantum electrodynamics in the ultrastrong coupling regime, *Nat. Phys.* 6(10), 772 (2010)
8. F. Yoshihara, T. Fuse, S. Ashhab, K. Kakuyanagi, S. Saito, and K. Semba, Superconducting qubit-oscillator circuit beyond the ultrastrong-coupling regime, *Nat. Phys.* 13(1), 44 (2017)
9. Y. H. Lin, L. B. Nguyen, N. Grabon, J. S. Miguel, N. Pankratova, and V. E. Manucharyan, Demonstration of protection of a superconducting qubit from energy decay, *Phys. Rev. Lett.* 120, 150503 (2018)
10. C. P. Yang, S. I. Chu, and S. Han, Quantum information transfer and entanglement with SQUID qubits in cavity QED: A dark-state scheme with tolerance for nonuniform device parameter, *Phys. Rev. Lett.* 92(11), 117902 (2004)

11. Z. Kis and E. Paspalakis, Arbitrary rotation and entanglement of flux SQUID qubits, *Phys. Rev. B* 69(2), 024510 (2004)
12. F. W. Strauch and C. J. Williams, Theoretical analysis of perfect quantum state transfer with superconducting qubits, *Phys. Rev. B* 78(9), 094516 (2008)
13. C. P. Yang, Quantum information transfer with superconducting flux qubits coupled to a resonator, *Phys. Rev. A* 82(5), 054303 (2010)
14. F. Mei, G. Chen, L. Tian, S. L. Zhu, and S. Jia, Robust quantum state transfer via topological edge states in superconducting qubit chains, *Phys. Rev. A* 98(1), 012331 (2018)
15. M. A. Sillanpää, J. I. Park, and R. W. Simmonds, Coherent quantum state storage and transfer between two phase qubits via a resonant cavity, *Nature* 449(7161), 438 (2007)
16. X. Li, Y. Ma, J. Han, T. Chen, Y. Xu, W. Cai, H. Wang, Y. P. Song, Z. Y. Xue, Z. Q. Yin, and L. Sun, Perfect quantum state transfer in a superconducting qubit chain with parametrically tunable couplings, *Phys. Rev. Appl.* 10(5), 054009 (2018)
17. C. P. Yang and S. Han, Preparation of Greenberger–Horne–Zeilinger entangled states with multiple superconducting quantum-interference device qubits or atoms in cavity QED, *Phys. Rev. A* 70(6), 062323 (2004)
18. S. L. Zhu, Z. D. Wang, and P. Zanardi, Geometric quantum computation and multiqubit entanglement with superconducting qubits inside a cavity, *Phys. Rev. Lett.* 94(10), 100502 (2005)
19. K. H. Song, Z. W. Zhou, and G. C. Guo, Quantum logic gate operation and entanglement with superconducting quantum interference devices in a cavity via a Raman transition, *Phys. Rev. A* 71(5), 052310 (2005)
20. T. Tanamoto, Y. Liu, S. Fujita, X. Hu, and F. Nori, Producing cluster states in charge qubits and flux qubits, *Phys. Rev. Lett.* 97(23), 230501 (2006)
21. X. L. Zhang, K. L. Gao, and M. Feng, Preparation of cluster states and W states with superconducting quantum-interference-device qubits in cavity QED, *Phys. Rev. A* 74(2), 024303 (2006)
22. J. Q. You, X. Wang, T. Tanamoto, and F. Nori, Efficient one-step generation of large cluster states with solid-state circuits, *Phys. Rev. A* 75(5), 052319 (2007)
23. Y. D. Wang, S. Chesi, D. Loss, and C. Bruder, One-step multiqubit Greenberger–Horne–Zeilinger state generation in a circuit QED system, *Phys. Rev. B* 81(10), 104524 (2010)
24. C. P. Yang, Preparation of n-qubit Greenberger–Horne–Zeilinger entangled states in cavity QED: An approach with tolerance to nonidentical qubit-cavity coupling constants, *Phys. Rev. A* 83(6), 062302 (2011)
25. W. Feng, P. Wang, X. Ding, L. Xu, and X. Q. Li, Generating and stabilizing the Greenberger–Horne–Zeilinger state in circuit QED: Joint measurement, Zeno effect, and feedback, *Phys. Rev. A* 83(4), 042313 (2011)
26. S. Aldana, Y. D. Wang, and C. Bruder, Greenberger–Horne–Zeilinger generation protocol for N superconducting transmon qubits capacitively coupled to a quantum bus, *Phys. Rev. B* 84(13), 134519 (2011)
27. T. Liu, Q. P. Su, S. J. Xiong, J. M. Liu, C. P. Yang, and F. Nori, Generation of a macroscopic entangled coherent state using quantum memories in circuit QED, *Sci. Rep.* 6(1), 32004 (2016)
28. C. P. Yang, Q. P. Su, S. B. Zheng, and F. Nori, Entangling superconducting qubits in a multi-cavity system, *New J. Phys.* 18(1), 013025 (2016)
29. Y. H. Kang, Y. H. Chen, Z. C. Shi, J. Song, and Y. Xia, Fast preparation of W states with superconducting quantum interference devices by using dressed states, *Phys. Rev. A* 94(5), 052311 (2016)
30. X. T. Mo and Z. Y. Xue, Single-step multipartite entangled states generation from coupled circuit cavities, *Front. Phys.* 14(3), 31602 (2019)
31. T. Liu, Q. P. Su, Y. Zhang, Y. L. Fang, and C. P. Yang, Generation of quantum entangled states of multiple groups of qubits distributed in multiple cavities, *Phys. Rev. A* 101(1), 012337 (2020)
32. C. Song, K. Xu, W. Liu, C. Yang, S. B. Zheng, H. Deng, Q. Xie, K. Huang, Q. Guo, L. Zhang, P. Zhang, D. Xu, D. Zheng, X. Zhu, H. Wang, Y. A. Chen, C. Y. Lu, S. Han, and J. W. Pan, 10-qubit entanglement and parallel logic operations with a superconducting circuit, *Phys. Rev. Lett.* 119(18), 180511 (2017)
33. M. Gong, M. C. Chen, Y. Zheng, S. Wang, C. Zha, H. Deng, Z. Yan, H. Rong, Y. Wu, S. Li, F. Chen, Y. Zhao, F. Liang, J. Lin, Y. Xu, C. Guo, L. Sun, A. D. Castellano, H. Wang, C. Peng, C. Y. Lu, X. Zhu, and J. W. Pan, Genuine 12-qubit entanglement on a superconducting quantum processor, *Phys. Rev. Lett.* 122(11), 110501 (2019)
34. C. Song, K. Xu, H. Li, Y. R. Zhang, X. Zhang, W. Liu, Q. Guo, Z. Wang, W. Ren, J. Hao, H. Feng, H. Fan, D. Zheng, D. W. Wang, H. Wang, and S. Y. Zhu, Generation of multicomponent atomic Schrödinger cat states of up to 20 qubits, *Science* 365(6453), 574 (2019)
35. A. Romanenko, R. Pilipenko, S. Zorzetti, D. Frolov, M. Awida, S. Belomestnykh, S. Posen, and A. Grassellino, Three-dimensional superconducting resonators at $T < 20$ mK with photon lifetimes up to $\tau = 2$ s, *Phys. Rev. Appl.* 13(3), 034032 (2020)
36. M. Mariantoni, F. Deppe, A. Marx, R. Gross, F. K. Wilhelm, and E. Solano, Two-resonator circuit quantum electrodynamics: A superconducting quantum switch, *Phys. Rev. B* 78(10), 104508 (2008)
37. S. T. Merkel and F. K. Wilhelm, Generation and detection of NOON states in superconducting circuits, *New J. Phys.* 12(9), 093036 (2010)
38. F. W. Strauch, K. Jacobs, and R. W. Simmonds, Arbitrary control of entanglement between two superconducting resonators, *Phys. Rev. Lett.* 105(5), 050501 (2010)
39. Y. Hu and L. Tian, Deterministic generation of entangled photons in superconducting resonator arrays, *Phys. Rev. Lett.* 106(25), 257002 (2011)
40. C. P. Yang, Q. P. Su, and S. Han, Generation of Greenberger–Horne–Zeilinger entangled states of photons in multiple cavities via a superconducting qutrit or an atom through resonant interaction, *Phys. Rev. A* 86(2), 022329 (2012)

41. P. B. Li, S. Y. Gao, and F. L. Li, Engineering two-mode entangled states between two superconducting resonators by dissipation, *Phys. Rev. A* 86(1), 012318 (2012)
42. C. P. Yang, Q. P. Su, S. B. Zheng, and S. Han, Generating entanglement between microwave photons and qubits in multiple cavities coupled by a superconducting qutrit, *Phys. Rev. A* 87(2), 022320 (2013)
43. S. J. Xiong, Z. Sun, J. M. Liu, T. Liu, and C. P. Yang, Efficient scheme for generation of photonic NOON states in circuit QED, *Opt. Lett.* 40(10), 2221 (2015)
44. R. Sharma and F. W. Strauch, Quantum state synthesis of superconducting resonators, *Phys. Rev. A* 93(1), 012342 (2016)
45. Z. Li, S. Ma, Z. P. Yang, A. P. Fang, P. Li, S. Y. Gao, and F. L. Li, Generation and replication of continuous-variable quadripartite cluster and Greenberger–Horne–Zeilinger states in four chains of superconducting transmission line resonators, *Phys. Rev. A* 93(4), 042305 (2016)
46. Y. J. Zhao, C. Q. Wang, X. B. Zhu, and Y. X. Liu, Engineering entangled microwave photon states through multiphoton interactions between two cavity fields and a superconducting qubit, *Sci. Rep.* 6(1), 23646 (2016)
47. Q. P. Su, H. H. Zhu, L. Yu, Y. Zhang, S. J. Xiong, J. M. Liu, and C. P. Yang, Generating double NOON states of photons in circuit QED, *Phys. Rev. A* 95(2), 022339 (2017)
48. C. P. Yang and Z. F. Zheng, Deterministic generation of Greenberger–Horne–Zeilinger entangled states of cat-state qubits in circuit QED, *Opt. Lett.* 43(20), 5126 (2018)
49. M. Li, M. Hua, M. Zhang, and F. G. Deng, Entangling two high-Q microwave resonators assisted by a resonator terminated with SQUIDs, *New J. Phys.* 21(7), 073025 (2019)
50. T. Liu, Y. Zhang, B. Q. Guo, C. S. Yu, and W. N. Zhang, Creation of superposition of arbitrary states encoded in two high-Q cavities, *Opt. Express* 27(19), 27168 (2019)
51. Y. Zhang, T. Liu, J. Zhao, Y. Yu, and C. P. Yang, Generation of hybrid Greenberger–Horne–Zeilinger entangled states of particlelike and wavelike optical qubits in circuit QED, *Phys. Rev. A* 101(6), 062334 (2020)
52. M. Hofheinz, E. M. Weig, M. Ansmann, R. C. Bialczak, E. Lucero, M. Neeley, A. D. O'Connell, H. Wang, J. M. Martinis, and A. N. Cleland, Generation of Fock states in a superconducting quantum circuit, *Nature* 454(7202), 310 (2008)
53. B. Vlastakis, G. Kirchmair, Z. Leghtas, S. E. Nigg, L. Frunzio, S. M. Girvin, M. Mirrahimi, M. H. Devoret, and R. J. Schoelkopf, Deterministically encoding quantum information using 100-Photon Schröinger cat states, *Science* 342(6158), 607 (2013)
54. C. Wang, Y. Y. Gao, P. Reinhold, R. W. Heeres, N. Ofek, K. Chou, C. Axline, M. Reagor, J. Blumoff, K. M. Sliwa, L. Frunzio, S. M. Girvin, L. Jiang, M. Mirrahimi, M. H. Devoret, and R. J. Schoelkopf, A Schrödinger cat living in two boxes, *Science* 352(6289), 1087 (2016)
55. H. Wang, M. Mariantoni, R. C. Bialczak, M. Lenander, E. Lucero, M. Neeley, A. D. O'Connell, D. Sank, M. Weides, J. Wenner, T. Yamamoto, Y. Yin, J. Zhao, J. M. Martinis, and A. N. Cleland, Deterministic entanglement of photons in two superconducting microwave resonators, *Phys. Rev. Lett.* 106(6), 060401 (2011)
56. A. Karlsson and M. Bourennane, Quantum teleportation using three-particle entanglement, *Phys. Rev. A* 58(6), 4394 (1998)
57. D. P. DiVincenzo and P. W. Shor, Fault-tolerant error correction with efficient quantum codes, *Phys. Rev. Lett.* 77(15), 3260 (1996)
58. V. Giovannetti, S. Lloyd, and L. Maccone, Quantum-enhanced measurements: Beating the standard quantum limit, *Science* 306(5700), 1330 (2004)
59. X. Wang, Quantum teleportation of entangled coherent states, *Phys. Rev. A* 64(2), 022302 (2001)
60. H. Jeong and M. S. Kim, Efficient quantum computation using coherent states, *Phys. Rev. A* 65(4), 042305 (2002)
61. J. Joo, W. J. Munro, and T. P. Spiller, Quantum metrology with entangled coherent states, *Phys. Rev. Lett.* 107(8), 083601 (2011)
62. P. T. Cochrane, G. J. Milburn, and W. J. Munro, Macroscopically distinct quantumsuperposition states as a bosonic code for amplitude damping, *Phys. Rev. A* 59(4), 2631 (1999)
63. Q. C. Wu, Y. H. Zhou, B. L. Ye, T. Liu, and C. P. Yang, Nonadiabatic quantum state engineering by time-dependent decoherence-free subspaces in open quantum systems, *New J. Phys.* 23(11), 113005 (2021)
64. H. Jeong and N. B. An, Greenberger–Horne–Zeilinger-type and *W*-type entangled coherent states: Generation and Bell-type inequality tests without photon counting, *Phys. Rev. A* 74(2), 022104 (2006)
65. A. Blais, S. M. Girvin, and W. D. Oliver, Quantum information processing and quantum optics with circuit quantum electrodynamics, *Nat. Phys.* 16(3), 247 (2020)
66. W. Cai, Y. Ma, W. Wang, C. L. Zou, and L. Sun, Bosonic quantum error correction codes in superconducting quantum circuits, *Fundamental Research* 1(1), 50 (2021)
67. D. Gottesman, A. Kitaev, and J. Preskill, Encoding a qubit in an oscillator, *Phys. Rev. A* 64(1), 012310 (2001)
68. N. Ofek, A. Petrenko, R. Heeres, P. Reinhold, Z. Leghtas, B. Vlastakis, Y. Liu, L. Frunzio, S. M. Girvin, L. Jiang, M. Mirrahimi, M. H. Devoret, and R. J. Schoelkopf, Extending the lifetime of a quantum bit with error correction in superconducting circuits, *Nature* 536(7617), 441 (2016)
69. M. H. Michael, M. Silveri, R. T. Brierley, V. V. Albert, J. Salmilehto, L. Jiang, and S. M. Girvin, New class of quantum error-correcting codes for a bosonic mode, *Phys. Rev. X* 6(3), 031006 (2016)
70. L. Hu, Y. Ma, W. Cai, X. Mu, Y. Xu, W. Wang, Y. Wu, H. Wang, Y. P. Song, C. L. Zou, S. M. Girvin, L. M. Duan, and L. Sun, Quantum error correction and universal gate set operation on a binomial bosonic logical qubit, *Nat. Phys.* 15(5), 503 (2019)
71. A. Sørensen and K. Mølmer, Quantum computation with ions in thermal motion, *Phys. Rev. Lett.* 82(9), 1971 (1999)
72. S. B. Zheng and G. C. Guo, Efficient scheme for two-atom entanglement and quantum information processing in cavity QED, *Phys. Rev. Lett.* 85(11), 2392 (2000)
73. D. F. James and J. Jerke, Effective Hamiltonian theory and its applications in quantum information, *Can. J. Phys.* 85(6), 625 (2007)

74. Y. Xu, Y. Ma, W. Cai, X. Mu, W. Dai, W. Wang, L. Hu, X. Li, J. Han, H. Wang, Y. Song, Z. B. Yang, S. B. Zheng, and L. Sun, Demonstration of controlled-phase gates between two error-correctable photonic qubits, *Phys. Rev. Lett.* 124(12), 120501 (2020)
75. M. Sandberg, C. M. Wilson, F. Persson, T. Bauch, G. Johansson, V. Shumeiko, T. Duty, and P. Delsing, Tuning the field in a microwave resonator faster than the photon lifetime, *Appl. Phys. Lett.* 92(20), 203501 (2008)
76. Z. L. Wang, Y. P. Zhong, L. J. He, H. Wang, J. M. Martinis, A. N. Cleland, and Q. W. Xie, Quantum state characterization of a fast tunable superconducting resonator, *Appl. Phys. Lett.* 102(16), 163503 (2013)
77. M. Scully and M. S. Zubairy, Quantum optics, Cambridge University Press, Cambridge, 1997, Chapter 2
78. G. Kirchmair, B. Vlastakis, Z. Leghtas, S. E. Nigg, H. Paik, E. Ginossar, M. Mirrahimi, L. Frunzio, S. M. Girvin, and R. J. Schoelkopf, Observation of quantum state collapse and revival due to the single-photon Kerr effect, *Nature* 495(7440), 205 (2013)
79. J. Koch, T. M. Yu, J. Gambetta, A. A. Houck, D. I. Schuster, J. Majer, A. Blais, M. H. Devoret, S. M. Girvin, and R. J. Schoelkopf, Charge-insensitive qubit design derived from the Cooper pair box, *Phys. Rev. A* 76(4), 042319 (2007)
80. I. C. Hoi, C. M. Wilson, G. Johansson, T. Palomaki, B. Peropadre, and P. Delsing, Demonstration of a single-photon router in the microwave regime, *Phys. Rev. Lett.* 107(7), 073601 (2011)
81. M. Fitzpatrick, N. M. Sundaresan, A. C. Y. Li, J. Koch, and A. A. Houck, Observation of a dissipative phase transition in a one-dimensional circuit QED lattice, *Phys. Rev. X* 7(1), 011016 (2017)
82. T. Liu, Z. F. Zheng, Y. Zhang, Y. L. Fang, and C. P. Yang, Transferring entangled states of photonic cat-state qubits in circuit QED, *Front. Phys.* 15(2), 21603 (2020)
83. J. B. Chang, M. R. Vissers, A. D. Córcoles, M. Sandberg, J. Gao, D. W. Abraham, J. M. Chow, J. M. Gambetta, M. Beth Rothwell, G. A. Keefe, M. Steffen, and D. P. Pappas, Improved superconducting qubit coherence using titanium nitride, *Appl. Phys. Lett.* 103(1), 012602 (2013)
84. A. P. M. Place, L. V. H. Rodgers, P. Mundada, B. M. Smitham, M. Fitzpatrick, Z. Leng, A. Premkumar, J. Bryon, S. Sussman, G. Cheng, et al., New material platform for superconducting transmon qubits with coherence times exceeding 0.3 milliseconds, arXiv: 2003.00024 (2020)
85. A. Megrant, C. Neill, R. Barends, B. Chiaro, Y. Chen, L. Feigl, J. Kelly, E. Lucero, M. Mariantoni, P. J. J. O'Malley, D. Sank, A. Vainsencher, J. Wenner, T. C. White, Y. Yin, J. Zhao, C. J. Palmstrøm, J. M. Martinis, and A. N. Cleland, Planar superconducting resonators with internal quality factors above one million, *Appl. Phys. Lett.* 100(11), 113510 (2012)
86. P. W. Woods, G. Calusine, A. Melville, A. Sevi, E. Golden, D. K. Kim, D. Rosenberg, J. L. Yoder, and W. D. Oliver, Determining interface dielectric losses in superconducting coplanar waveguide resonators, *Phys. Rev. Appl.* 12(1), 014012 (2019)